

# Superplasticity in cubic yttria stabilized zirconia with 10 wt.% alumina

Adel A. Sharif<sup>a,\*</sup>, Martha L. Mecartney<sup>b</sup>

<sup>a</sup>Department of Mechanical Engineering, California State University, 5151 State University Drive, Los Angeles, CA 90032-8153, USA

<sup>b</sup>Department of Chemical and Biochemical Engineering & Materials Science, University of California, Irvine, CA, 92697-2575, USA

Received 21 November 2002; received in revised form 15 May 2003; accepted 1 June 2003

## Abstract

The feasibility of superplasticity in 8 mol% cubic yttria stabilized zirconia (8Y-CSZ) containing a fine dispersion of alumina was investigated. Grain growth of 8Y-CSZ was limited by addition of 1–10 wt.% alumina. A fine grain size on the order of 1.1  $\mu\text{m}$  was achieved with a dispersion of 10 wt.% alumina in 8Y-CSZ. Deformation tests under compression were conducted at temperatures from 1300 to 1450 °C for 8Y-CSZ with 10 wt.% alumina. Strain rates as high as  $4 \times 10^{-3} \text{ s}^{-1}$  at 1450 °C were obtained, similar to the high strain rates observed for superplastic tetragonal yttria stabilized zirconia. The inverse grain-size exponent and the stress exponent both were calculated to be around 2 and the activation energy for high temperature deformation was calculated to be in the range of 597–683 kJ/mol.

© 2003 Elsevier Ltd. All rights reserved.

**Keywords:** Creep; Cubic zirconia; Superplasticity;  $\text{ZrO}_2$

## 1. Introduction

Difficulties involved with shape forming of ceramics can be a barrier to cost effective use of these materials. Superplastic deformation, defined as extensive uniform deformation at high temperatures, is an attractive route for net shape forming. The microstructural design of superplastic ceramics requires an ultrafine grain size that is stable against coarsening during sintering and high-temperature deformation.<sup>1–3</sup> Only a few ceramics, however, such as yttria stabilized tetragonal zirconia polycrystals (Y-TZP) have the fine grain size ( $< 1 \mu\text{m}$ ) and sluggish grain growth rate required for superplastic deformation. In general, most ceramics have rapid grain growth rates at the high temperatures required for deformation, making them unsuitable for superplastic deformation.

Cubic yttria stabilized zirconia (Y-CSZ) is a typical oxide ceramic with a larger grain size ( $> 10 \mu\text{m}$ ) and a higher grain growth rate than Y-TZP (30–250 times).<sup>4,5</sup> Y-CSZ is a stable single-phase material formed with

higher concentrations of yttria ( $\text{Y}_2\text{O}_3$ ) in solid solution with zirconia ( $\text{ZrO}_2$ ) than Y-TZP.<sup>6</sup> Y-CSZ, with its high oxygen diffusion coefficient, low electronic conductivity, and excellent chemical stability under reducing and oxidizing atmospheres at high temperatures, has found application as a high performance solid electrolyte in high temperature electrochemical devices and solid oxide fuel cells.<sup>7–9</sup>

Due to rapid static and dynamic grain growth during synthesis and high temperature deformation, superplasticity has not been observed in Y-CSZ ceramics. Dynamic grain growth is the stress induced accelerated grain growth during deformation when compared to static grain growth at the same temperature without an imposed stress.<sup>10</sup> The ability to limit grain growth is a critical problem for superplastic forming. Even when a fine grain material can be synthesized, rapid grain growth during high temperature deformation lowers the strain rate during superplastic deformation<sup>3,10</sup>. Particularly at low strain rates, when the sample is exposed to high temperatures for long times, strain hardening becomes significant. In materials with rapid dynamic grain growth rates such as 8 mol% yttria stabilized cubic zirconia (8Y-CSZ), the effect of strain hardening can be significant after only a few minutes.

\* Corresponding author. Tel.: +1-323-3434478; fax: +1-323-3435004.

E-mail address: [aasharif@calstatela.edu](mailto:aasharif@calstatela.edu) (A.A. Sharif).

Thus, in order to achieve the high strain rates required for superplastic deformation of Y-CSZ, it is necessary to limit intrinsic grain growth during sintering and prevent dynamic grain growth during high temperature deformation. The use of an intergranular or a second phase to pin the grain boundaries and limit grain growth has been successfully applied in metallic systems to facilitate superplastic deformation.<sup>11</sup> In ceramic systems, particles of ZrO<sub>2</sub>, HfO<sub>2</sub>, and TiO<sub>2</sub> have been used in alumina and mullite to limit dynamic grain growth and promote a high temperature deformation rate.<sup>12–17</sup> Xue and Chen<sup>15</sup> observed that by adding zirconia to alumina, not only there was a suppression of grain growth, but also cavitation nucleation was prevented during high temperature deformation.

Alumina has been used effectively as a pinning agent in other zirconia systems.<sup>18–23</sup> Y-TZP containing 20 wt.% alumina exhibits considerably less dynamic grain growth than pure Y-TZP.<sup>19</sup> It has been found that additions of alumina result in higher ductility during high temperature tensile elongation of 3Y-TZP<sup>19,24</sup> and 5.5YSZ.<sup>25</sup> Furthermore, addition of alumina to 8Y-CSZ improves the ionic conductivity of impure ceramics<sup>26–28</sup> and increases strength and thermal shock of YSZ.<sup>9,29</sup>

Since grain size is the most important parameter affecting superplasticity in ceramics, the emphasis of this investigation was placed on controlling grain growth. The first step of this research was to study the effect of addition of fine particle size (<0.3 μm) alumina on grain growth of 8Y-CSZ. After fabricating samples of 8Y-CSZ/alumina with limited grain growth, the high temperature deformation behavior of these samples was characterized. This research uses 8Y-CSZ as a model system to investigate the effectiveness of an inert second phase in promoting superplasticity in a ceramic that does not normally demonstrate superplastic behavior due to grain growth.

## 2. Experimental procedures

Commercially available 8Y-CSZ powder with a particle size of 24 nm (Tosoh, Japan) was used to prepare samples with no additives (hereafter called “pure samples”) and samples with 1, 5, and 10 wt.% (1.5, 7.3, and 14 vol.%, respectively) alumina with a particle size of <0.3 μm (Alfa Products, MA). Right circular cylinders of nearly full density were made from these powders by hot isostatic pressing at 1400 °C as described elsewhere.<sup>30</sup> For grain growth studies, samples were polished down to 0.05 μm, ultrasonically cleaned in acetone and methanol, and placed in a rapid-heating box furnace for annealing times of 3, 10, 25, 50, 75, and 100 h in air at 1400 °C. A heating rate of 100 °C per minute was used. The samples were cooled to room temperature inside the furnace.

Scanning electron microscopy (Philips XL 30 FEG) was used to obtain photomicrographs from the thermally etched surfaces of the sample which were polished prior to being placed in the furnace for grain growth. The conventional mean linear intercept method was used on the photomicrographs to calculate the grain size. The reported grain size values are the average intercept length multiplied by 1.74.<sup>31</sup>

Samples for creep experiments were prepared with a diameter of 2.5 mm and a height of 5 mm. A right angular fixture was used to polish the sample ends perpendicular to the sample surface and parallel to each other. High temperature deformation of these samples at the temperature range of 1300–1500 °C was accomplished in a compression creep furnace (ATS, Inc. PA) between two SiC rods under quasi-constant stress conditions. Assuming a uniform diameter throughout the samples, increase in the cross sectional area was calculated for increments of decrease in sample height. A chart was prepared correlating the extensometer reading to stress. This chart was used during the experiment to adjust the load on the creep machine manually to keep the stress nearly constant, checking after each 0.01 increment of strain. For all experiments, the creep furnace reached the testing temperatures in 3 h.

## 3. Results

The typical rapid static grain growth of pure 8Y-CSZ is illustrated in Fig. 1. Although the 8Y-CSZ samples had an initial grain size of 3 μm, after annealing for 75 h at 1400 °C the grains grew to about 11 μm (Fig. 1). The effect of addition of various amounts of Al<sub>2</sub>O<sub>3</sub> on static grain growth is shown in Fig. 2. Addition of only 1 wt.% alumina had little effect on limiting static grain growth; however, increasing the amount of alumina resulted in a smaller initial grain size and a more limited static grain growth. Samples containing 10 wt.% alumina had an initial grain size of about 1.1 μm after fabrication that grew to about 2.5 μm after annealing for 75 h at 1400 °C (Fig. 3), five times smaller than pure 8Y-CSZ (Fig. 1).

High-temperature compressive deformation of samples containing 10 wt.% alumina resulted in a relatively uniform deformation for samples deformed at stresses below 35 MPa and at temperatures above 1300 °C. An example of this uniform deformation at 1450 °C and 10 MPa is shown in Fig. 4. A 130% true strain (260% engineering strain) was obtained at 1450 °C before the test was stopped. At lower temperatures below 1300 °C and stresses above 35 MPa, deformation was not always uniform; some samples deformed to a barrel shape and often fractured.

Some surface cracks were observed on samples undergone extensive deformation. Cracks observed on

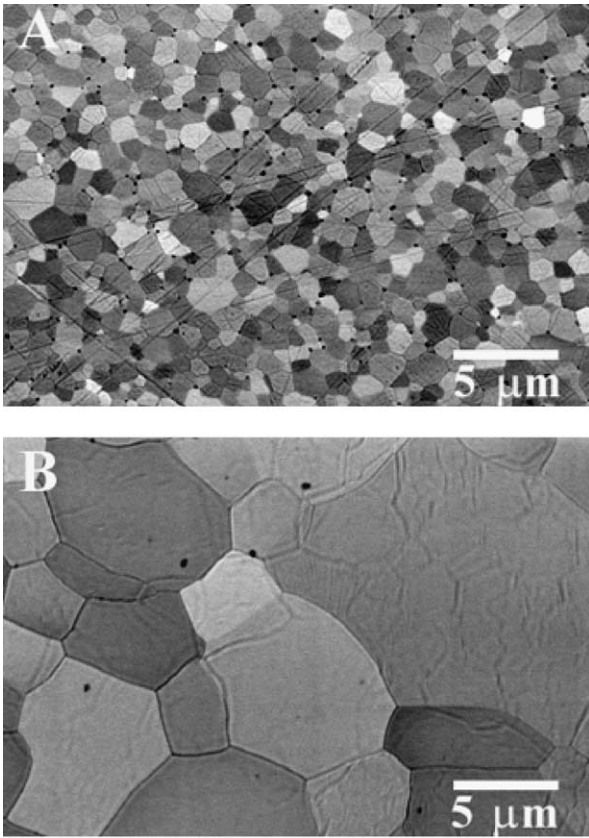


Fig. 1. Rapid static grain growth in 8Y-CSZ, (a) as hot isostatically pressed and (b) after annealing statically for 75 h at 1400 °C.

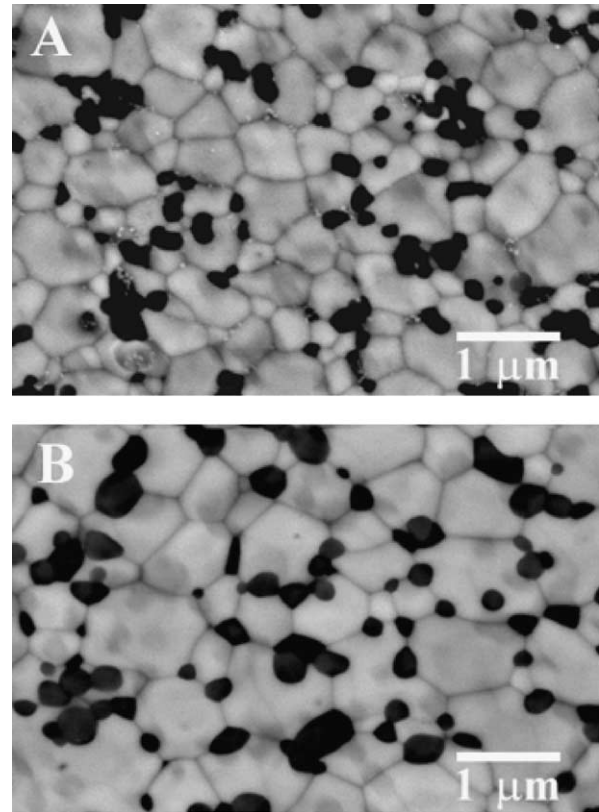


Fig. 3. Effect of addition of 10 wt.% alumina on static grain growth of 8Y-CSZ (a) as hot-isostatically pressed and (b) after annealing statically for 75 h at 1400 °C.

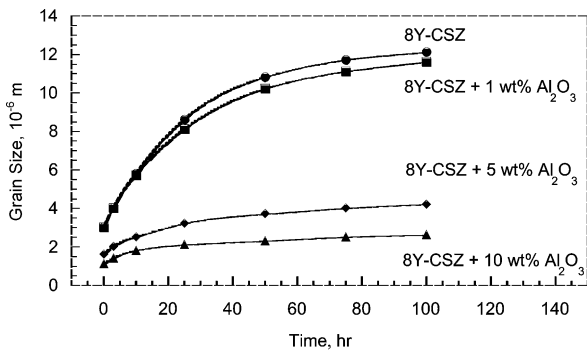


Fig. 2. Effect of addition of various amounts of alumina on static grain growth of 8Y-CSZ at 1400 °C.

the surfaces of the samples parallel to the direction of the stress and microcracks on the sample surfaces facing the platen. However, these surface cracks did not penetrate beyond about 50 μm and they were not likely to have a significant effect on deformation behavior under compression. No cracks or fractures could be found in the interior of uniformly deformed samples.

Deformation at high temperatures resulted in some dynamic grain growth for samples that had undergone large deformations (Fig. 5). It was observed that strain hardening at constant stress and constant temperature

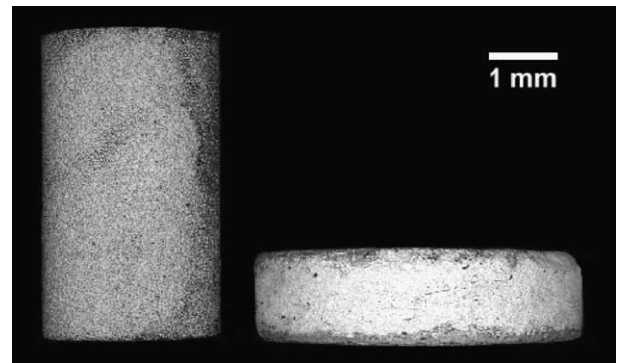


Fig. 4. 8Y-CSZ + 10 wt.% alumina samples before and after creep at 1450 °C, 10 MPa.

was much less significant in samples containing 10 wt.% alumina when compared to pure 8Y-CSZ samples.

The dependence of strain rate on grain-size can be calculated from:

$$\dot{\epsilon} = A d^{-p} \sigma^n \exp\left(\frac{-Q}{RT}\right) \quad (1)$$

where  $\dot{\epsilon}$  denotes steady state strain rate,  $A$  is a constant,  $d$  is the grain size,  $p$  is the inverse grain size exponent,  $\sigma$  is the applied stress,  $n$  is the stress exponent,  $Q$  is the activation energy for the rate controlling deformation

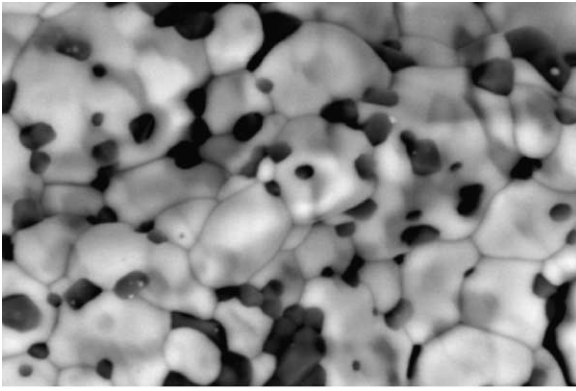


Fig. 5. Grain growth for 8Y-CSZ + 10 wt.% alumina after total true strain of 115% at 1400 °C, 25 MPa.

mechanism,  $R$  is the gas constant, and  $T$  is the absolute temperature. The inverse grain size exponent,  $p$ , may be calculated from the slope of the line obtained by plotting  $\dot{\epsilon}$  vs.  $d$  in logarithmic scale. A value of 2.2 was calculated for  $p$  from strain rates obtained for three samples with different initial grain sizes as shown in Fig. 6. The stress exponent,  $n$ , was calculated from the slope of the straight line obtained by plotting  $\dot{\epsilon}$  vs.  $\sigma$  in logarithmic scale as shown in Fig. 7. The values of strain rate,  $\dot{\epsilon}$ , throughout these calculations were done on nearly isostrain segments of the strain vs. time curve obtained during high-temperature deformation that was a straight line. The stress exponent was observed to decrease with increasing temperature from 2.1 at 1300 °C to 1.7 at 1450 °C as shown in Fig. 7.

The slope of the straight line obtained from an Arrhenius type plot of strain rate vs. inverse absolute temperature was used to determine the activation energy for high-temperature deformation at constant stress (Fig. 8). The values of the activation energies calculated here are ranging from 683 kJ/mol at 10 MPa to

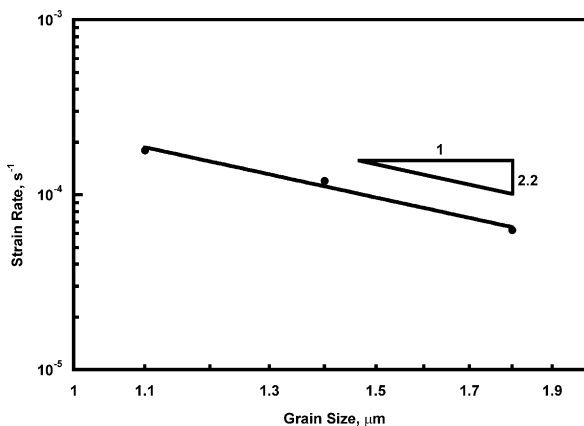


Fig. 6. Effect of grain size on steady state strain rate of 8Y-CSZ + 10 wt.% alumina at 1400 °C, 20 MPa.

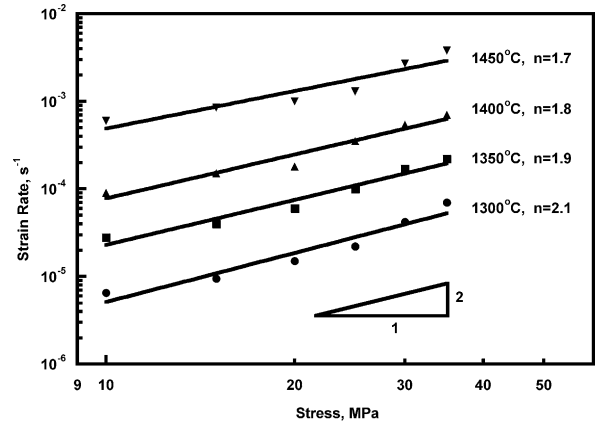


Fig. 7. Calculation of stress exponent for creep of 8Y-CSZ + 10 wt.% alumina at 1300–1450 °C.

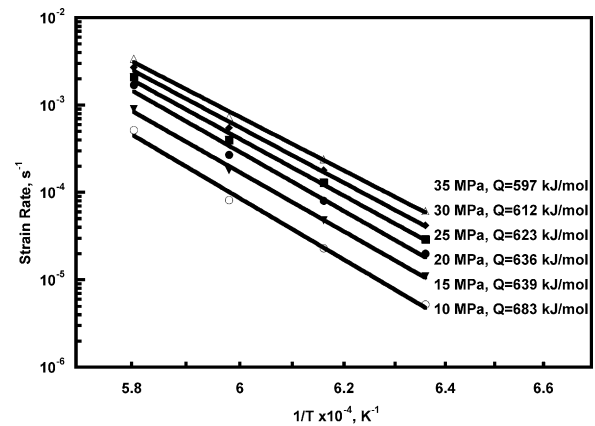


Fig. 8. Arrhenius type plot for creep of 8Y-CSZ + 10 wt.% alumina at 10–35 MPa.

597 kJ/mol at 35 MPa. A decrease in activation energy was observed by increasing stress.

## 4. Discussion

### 4.1. Limiting grain growth

To achieve effective grain boundary pinning, it is necessary for the grain corners to be pinned in more than half the multiple junctions. In two dimensions (2-D), for typical hexagonal grains such as those observed here (Fig. 3), a minimum of three alumina particles is necessary for an effective grain boundary pinning. In the presence of less than three particles per grain in 2-D, although the grain boundary movement is limited on one or two sides of the hexagon, the grain may grow on those sides, which are void of pinning agents. In reality, grains occupy a three-dimensional (3-D) space and may be represented by truncated octahedra (tetra-kaidecahedra) with 24 vertices and the analogy used for 2-D may be extended to 3-D. Mathematically, this is

described by various derivations of Zener Drag equation.<sup>32</sup> A modified Zener equation derived by Anderson et al.<sup>33</sup> from a 3-D computer simulation by Monte Carlo method describes the inhibiting effect of second phase particles on grain growth as:

$$\frac{d}{r} = 1.8f^{-0.33} \quad (2)$$

where  $d$  is the grain size of the pinned structure,  $r$  is the mean radius of second phase particles, and  $f$  is the volume fraction of second phase material.

From the initial grain size of 1.1  $\mu\text{m}$  and alumina average particle size of 0.3  $\mu\text{m}$ , ( $r=0.15 \mu\text{m}$ ), the minimum volume fraction of the secondary phase for an effective pinning is about 1.4 vol.% ( $\sim 1$  wt.%). However, as seen in Fig. 3, agglomeration of alumina particles results in a considerable decrease in the number of pinning particles. In the presence of 1 wt.% (1.5 vol.%) alumina, the rate of grain growth is only slightly smaller than those of pure samples (Fig. 2). As the amount of alumina is increased, grain growth is limited more effectively. This is expected since with increasing the volume fraction of alumina more multiple junctions are being occupied by alumina particles. With the addition of 10 wt.% ( $\sim 14$  vol.%) alumina, the grain size is predicted to be about 0.5  $\mu\text{m}$  from Eq. (2). The larger actual grain size of 1.1  $\mu\text{m}$  for the samples is due to the nonuniform distribution and agglomeration of alumina particles along the grain boundaries (Fig. 3). Under static annealing conditions, even at high temperatures and with long annealing times grain boundaries remained attached to pinning particles (Fig. 3b). Separation of grain boundaries from pinning particles was observed after extensive deformation (Fig. 5).

Although superplasticity in pure fine-grained ceramics is typically associated with a critical grain size of about 1  $\mu\text{m}$ , the 10 wt.% alumina 8Y-CSZ samples demonstrated extensive deformation and high strain rates even with larger grain size. Modification of the grain boundary chemistry and intergranular bonding may play a critical role. Alumina in cubic zirconia is known to change the grain boundary conductivity and structure,<sup>9,26,27</sup> which could influence grain boundary sliding and diffusion. Such a phenomenon was observed by Tsurui and Sakuma<sup>34</sup> who showed that although addition of 5 wt.%  $\text{TiO}_2$  to Y-TZP increased the grain size of the samples to 2.6  $\mu\text{m}$ , these samples could be deformed at 1500  $^\circ\text{C}$  at the same rate ( $1.3 \times 10^{-4} \text{ s}^{-1}$ ) as pure Y-TZP with a submicron grain size of 0.84  $\mu\text{m}$ . Further investigations are needed to elucidate the effect of grain boundary chemistry on deformation rate of ceramics.

#### 4.2. Cavity formation

In addition to sluggish grain growth and ease of grain boundary sliding, another prerequisite for a material to

exhibit extensive superplastic deformation is resistance to cavity formation. The presence of alumina has been observed to facilitate cavity formation in Y-TZP.<sup>35</sup> Excess cavity formation can be understood in terms of the relative size of the second phase inclusion. During deformation, tensile stress between adjacent grains and at multiple junctions creates a pressure gradient favorable for the particles to move towards that point. Small particles may become mobile in the presence of only small pressure gradients, whereas, large particles require larger pressure gradients to become mobile since the magnitude of the friction per particle increases by increasing particle size. Easy migration of small particles prevents cavity nucleation. In the absence of second phase mobility, the tensile stress results in cavity nucleation.

One of the most important characteristics of superplastic Y-TZP is its fine grain size ( $< 0.3 \mu\text{m}$ ). However, even fine particle alumina powder additions have a despersoid size equal or greater than 0.3  $\mu\text{m}$  due to powder agglomeration and lack of a perfectly-uniform particle distribution in the matrix. Hence, in Y-TZP the ratio of alumina particle size to grain size is relatively large and may even be greater than unity. On the other hand, the Y-CSZ used in this study has a much larger grain size (1.1  $\mu\text{m}$ ) than the alumina particle size (0.3  $\mu\text{m}$ ) and the ratio of alumina particle size to Y-CSZ grain size is much smaller than unity. This may explain why the formation of cavities in Y-CSZ in the presence of alumina particles is not observed as it is in Y-TZP ceramics with alumina inclusions.

#### 4.3. Deformation mechanism

The effect of grain size on strain rate is evident from Eq. (1). A higher value of  $p$  indicates a high sensitivity of strain rate on grain size. In fine grain oxides the reported values of  $p$  vary in the range of 1–3 depending on the rate controlling mechanism.<sup>20,36</sup> Values of 2 (Ref. 37) and 2–3 (Refs. 38 and 39) have been reported for inverse grain size exponent of pure cubic zirconia and pure alumina, respectively. Nieh and Wadsworth<sup>20</sup> found that the strain rate of 20 wt.% alumina reinforced Y-TZP was inversely proportional to  $d^{1.5}$ . The value of 2.2 calculated here falls well within the expected range, although towards the higher end.

The inverse of stress exponent ( $n$ ) is called strain rate sensitivity exponent ( $m$ ) and is a measure of ability of the material to undergo elongation without neck formation. Superplasticity is generally associated with  $m > 0.4$ .<sup>40</sup> The value of  $m$  varies from zero to unity. A Small value of  $m$  is an indication of easy neck formation during tensile deformation, hence, lack of superplasticity. In contrast, values of  $m$  close to 1 indicates resistance to flow localization and resistance to neck formation during tensile deformation, hence, the mate-

rial is able to undergo large tensile deformations. Since neck formation is the onset of failure during tensile deformation, for superplastic deformation it is desirable to have an  $m$  value as close to unity as possible. Since neck formation does not take place under compression, one may argue that the values obtained for  $m$  under compression are meaningless. However, the values of  $m$  were similar for 3Y-TZP in tension and compression.<sup>41</sup>

The values of  $m$  calculated from the inverse of  $n$  in Fig. 7 range from 0.48 at 1350 °C to 0.59 at 1450 °C. An increase in the value of  $m$  was observed with increasing temperature. Hence, it may be concluded that superplasticity in the ceramic is enhanced at higher temperatures. This indicates diffusion dependence of the rate controlling mechanism for deformation. In fine-grained ceramics, it has been proposed that superplasticity occurs with grain boundary sliding accommodated by a diffusional mechanism.<sup>42</sup> Diffusion accommodation is necessary during deformation to prevent cavity formation. In the absence of diffusion, as the grains slide passed each other, tensile stress concentration at triple junctions results in cavitation.

Activation energy was calculated at several stresses and it was found that the value of activation energy decreased by increasing stress. There was only a relatively small decrease in the magnitude of activation energy from 15 to 35 MPa (639–597 kJ/mol). However, a relatively large change in activation energy was observed for the change in stress from 10 to 15 MPa. It is possible that there was a change in deformation mechanism, which occurs at about 15 MPa. Clarisse et al.<sup>18</sup> also observed a stress dependence of activation energy and a decrease in activation energy with increasing stress. They attributed this behavior to be a consequence of two serial mechanisms accommodating grain boundary sliding, a high stress grain boundary diffusion accommodation and a low stress interface reaction accommodation. A reported activation energy of 633 kJ/mol for creep of 40 wt.% alumina/60 wt.% 8Y-CSZ composite at 75 MPa<sup>43</sup> is similar to the result obtained here for 10 wt.% alumina 90 wt.% 8Y-CSZ. These results are higher than some reported values (450–517 kJ/mol) of activation energy for creep of pure 8Y-CSZ.<sup>3,43</sup>

A comparison of the activation energy for superplastic deformation of this 8Y-CSZ containing 10 wt.% alumina (683–597 kJ/mol) to the activation energy for superplastic deformation of 3Y-TZP (640 kJ/mol) under identical experimental conditions<sup>41</sup> shows a surprisingly similar range of values. This indicates that without a major difference in grain size, the high temperature deformation behaviors of these two materials (8Y-CSZ/Al<sub>2</sub>O<sub>3</sub> and 3Y-TZP) are very similar. The same mechanism of grain boundary sliding accommodated by diffusional creep is operable in both cases. At both low and high stresses diffusion plays the role of the accommodator, at low stresses it accommodates interfacial

reaction controlled deformation and at high stresses it accommodates grain boundary sliding.

## 5. Summary

Addition of a fine dispersion of alumina to cubic 8Y-CSZ enables the ceramic to behave superplastically during high temperature deformation. Addition of 10 wt.% alumina to 8Y-CSZ resulted in a 1.1 μm grain size. Values of approximately 2 were calculated for the inverse grain size exponent and the stress exponent, similar to values reported for high temperature deformation of tetragonal 3Y-TZP. Strain rates as high as about  $4 \times 10^{-3} \text{ s}^{-1}$  at 1450 °C and activation energies for creep in the range of 597–683 kJ/mol were obtained. Total true strain of 130% true strain (260% engineering strain) was obtained at 1450 °C/10 MPa. Addition of finely dispersed inert phases, can be an effective approach for inducing superplasticity in oxide ceramics.

## Acknowledgements

Support for the experimental portion of the research was provided by the grant number STB-UC97-197 from the Collaborative UC/Los Alamos Research program. The purchase of the field emission scanning electron microscope was made possible through instrumentation grant DMR 9503774 from the NSF.

## References

- Nieh, T. G., McNally, C. M. and Wadsworth, J., Superplastic properties of a fine-grained yttria-stabilized tetragonal polycrystal of zirconia. *Scripta Metall.*, 1988, **22**, 1297–1300.
- Maehara, Y. and Langdon, T. G., Superplasticity of ceramics. *J. Mat. Sci.*, 1990, **25**, 2275–2286.
- Chen, I.-W. and Xue, L. A., Development of superplastic structural ceramics. *J. Am. Ceram. Soc.*, 1990, **73**, 2585–2609.
- Lee, I. G. and Chen, I.-W., Sintering and grain growth in tetragonal and cubic zirconia. In *Sintering 87*, ed. S. Somiya, M. Yoshimura and R. Watanabe. Elsevier, London, 1988, pp. 340–345.
- Yoshizawa, Y. I. and Sakuma, T., Evolution of microstructure and grain growth in ZrO<sub>2</sub>-Y<sub>2</sub>O<sub>3</sub> alloys. *ISIJ International*, 1989, **29**, 746–752.
- Scott, H. G., Phase relationship in the zirconia–yttria system. *J. Mat. Sci.*, 1975, **10**, 1527–1535.
- Glanz, G. and Zuda, A., Solid electrolyte fuel-cell based on stabilized zirconia. *Studii Si Cercetari De Fizica*, 1978, **30**, 31–54.
- Aoki, M., Chiang, Y.-M., Kosacki, I., Lee, L. J.-R., Tuller, H. and Liu, Y., Solute segregation and grain boundary impedance in high purity stabilized zirconia. *J. Am. Ceram. Soc.*, 1996, **79**, 1169–1180.
- Mori, M., Abe, T., Itoh, H., Yamamoto, O., Takeda, Y. and Kawahara, T., Cubic stabilized zirconia and alumina composites as electrolytes in planar type solid oxide fuel cells. *Solid State Ionics*, 1994, **74**, 157–164.

10. Nieh, T. G. and Wadsworth, J., Dynamic grain growth during superplastic deformation of yttria-stabilized tetragonal zirconia polycrystals. *J. Am. Ceram. Soc.*, 1989, **72**, 1469–1472.
11. Sherby, O. D. and Wadsworth, J., Superplasticity—recent advances and future directions. *Prog. Mater. Sci.*, 1989, **33**, 169–221.
12. Wang, J.-G. and Raj, R., Interface effects in superplastic deformation of alumina containing zirconia, titania or hafnia as a second phase. *Metall. Mater.*, 1991, **39**, 2909–2919.
13. Flacher, O., Blandin, J. J. and Plucknett, K. P., Effect of zirconia additions on superplasticity of alumina–zirconia composites. *Mater. Sci. Eng. A*, 1996, **221**, 102–112.
14. Nakano, K., Susuki, T. S., Hiraga, K. and Sakka, Y., Superplastic tensile ductility enhanced by grain size refinement in zirconia-dispersed alumina. *Scripta Mater.*, 1998, **38**, 33–38.
15. Xue, L. A. and Chen, I.-W., Superplastic alumina at temperatures below  $^{\circ}\text{C}$  using charge-compensating dopants. *J. Am. Ceram. Soc.*, 1996, **1300**, 79 233–238.
16. Xue, L. A., Wu, X. and Chen, I.-W., Superplastic alumina ceramics with grain growth inhibitors. *J. Am. Ceram. Soc.*, 1991, **74**, 842–845.
17. Yoon, C. K. and Chen, I.-W., Superplastic flow of two-phase ceramics containing rigid inclusions-zirconia/mullite composites. *J. Am. Ceram. Soc.*, 1990, **73**, 1555–1565.
18. Clarisse, L., Baddi, R., Bataille, A., Crampon, J., Duclos, R. and Vicens, J., Superplastic deformation mechanisms during creep of alumina–zirconia composites. *Acta Mat.*, 1997, **45**, 3843–3853.
19. Nieh, T. G., McNally, C. M. and Wadsworth, J., Superplastic behaviour of a 20%  $\text{Al}_2\text{O}_3/\text{YTZ}$  ceramic composite. *Scripta Metall.*, 1989, **23**, 457–460.
20. Nieh, T. G. and Wadsworth, J., Effect of grain size on superplastic behavior of  $\text{Al}_2\text{O}_3/\text{YTZ}$ . *J. Mater. Res.*, 1990, **5**, 2613–2615.
21. Okada, K. and Sakuma, T., Tensile ductility in zirconia-dispersed alumina at high temperatures. *J. Am. Ceram. Soc.*, 1996, **79**, 499–502.
22. Owen, D. M. and Chokshi, A. H., Observations of primary regions in the tensile creep deformation of superplastic zirconia–alumina composite. *Scripta Metall. Mater.*, 1993, **29**, 869–874.
23. Wakai, F. and Kato, H., Superplasticity of TZP/ $\text{Al}_2\text{O}_3$  ceramics. *Adv. Ceram. Mater.*, 1988, **3**, 71–76.
24. Wakai, F., Kato, H., Sakaguchi, S. and Murayama, N., Compressive deformation of  $\text{Y}_2\text{O}_3$ -stabilized  $\text{ZrO}_2/\text{Al}_2\text{O}_3$  composite. *J. Ceram. Soc. JPN*, 1986, **94**, 1017–1020.
25. Yamana, K., Nakamura, T., Yoshimura, K., Ina, K. and Weppner, W., Electrical resistance and deformation of yttria-stabilized cubic zirconia with alumina. *Solid State Ionics*, 1992, **53–56**, 763–768.
26. Susnik, D., Holc, J., Hrovat, M. and Zupancic, S., Influence of alumina addition on characteristics of cubic zirconia. *J. Mat. Sci. Lett.*, 1997, **16**, 1118–1120.
27. Mori, M., Yoshikawa, M., Itoh, H. and Abe, T., Effect of alumina on sintering behavior and electrical conductivity of high-purity yttria-stabilized zirconia. *J. Am. Ceram. Soc.*, 1994, **77**, 2217–2219.
28. Drennan, J., Swain, M. V. and Badwal, S. P. S., Anisotropic ionic conductivity observed in superplastically deformed yttria-stabilized zirconia/alumina composite. *J. Am. Ceram. Soc.*, 1989, **72**, 1279–1281.
29. Terauchi, S., Takizawa, H., Endo, T., Uchida, S., Terui, T. and Shimada, M., High ionic conductivity and high fracture strength of cubic zirconia,  $(\text{Y}_{0.16-x}\text{Sc}_x)\text{Zr}_{0.84}\text{O}_{1.92}$ /alumina composites. *Mater. Lett.*, 1995, **23**, 273–275.
30. Sharif, A. A., Imamura, P. H., Mitchell, T. E. and Mecartney, M. L., Control of grain growth using intergranular silicate phases in cubic yttria-stabilized zirconia. *Acta Mat.*, 1998, **46**, 3863–3872.
31. Thompson, A. W., Calculation of true volume grain diameter. *Metallography*, 1972, **5**, 366–369.
32. Smith, C. S., Grains, phases, and interfaces: an interpretation of microstructures. *Trans. AIME*, 1949, **175**, 15–23.
33. Anderson, M. P., Grest, G. S., Doherty, R. D. and Kang, L. I., Inhibition of grain growth by second phase particles: three dimensional Monte Carlo computer simulations. *Scripta Metall.*, 1989, **23**, 753–758.
34. Tsurui, K. and Sakuma, T., A unique role of  $\text{TiO}_2$  on the superplastic flow in tetragonal zirconia polycrystals. *Scripta Mater.*, 1996, **34**, 443–447.
35. Chokshi, A. H., Schissler, D. J., Nieh, T.-G. and Wadsworth, J., *A Comparative Study of Superplastic Deformation and Cavitation Failure in a Yttria Stabilized Zirconia and a Zirconia Alumina Composite*. MRS, San Francisco, CA, 1990.
36. Cannon, W. R. and Langdon, T. G., Creep of ceramics I: mechanical characteristics. *J. Mat. Sci.*, 1983, **18**, 1–50.
37. Evans, P. E., Creep in yttria- and scandia-stabilized zirconia. *J. Am. Ceram. Soc.*, 1970, **53**, 365–369.
38. Chokshi, A. H. and Porter, J. R., Analysis of concurrent grain growth during creep of polycrystalline alumina. *J. Am. Ceram. Soc.*, 1986, **69**, C37–39.
39. Cannon, R. M., Rhodes, W. H. and Heuer, A. H., Plastic deformation of fine grained alumina ( $\text{Al}_2\text{O}_3$ ): I, interface-controlled diffusional creep. *J. Am. Ceram. Soc.*, 1980, **63**, 46–58.
40. Pilling, J. and Ridley, N., *Superplasticity in Crystalline Solids*. Institute of Metals, Brookfield, VT, 1989.
41. Gust, M., Goo, G., Wolfenstine, J. and Mecartney, M., Influence of amorphous grain boundary phases on the superplastic behavior of 3-mol%-yttria-stabilized tetragonal zirconia polycrystals (3Y-TZP). *J. Am. Ceram. Soc.*, 1993, **76**, 1681–1690.
42. Ashby, M. F. and Verral, R. A., Diffusion-accommodated flow and superplasticity. *Acta Metall.*, 1973, **21**, 149–163.
43. French, J. D., Zhao, J., Harmer, M. P., Chan, H. M. and Miller, G. A., Creep of duplex microstructures. *J. Am. Ceram. Soc.*, 1994, **77**, 2857–2865.